Unexpected Toxicity of Monolayer Protected Gold Clusters Eliminated by PEG-Thiol Place Exchange Reactions

Carrie A. Simpson, Brian J. Huffman,[†] Aren E. Gerdon,[‡] and David E. Cliffel*

Department of Chemistry, Vanderbilt University, Nashville, Tennessee 37235

Received June 22, 2010

Monolayer protected clusters (MPCs) are small, metal nanoparticles capped with thiolate ligands that have been widely studied for their size-dependent properties and for their ability to be functionalized for biological applications. Common water-soluble MPCs, functionalized by *N*-(2-Mercaptopropionyl)-glycine (tiopronin) or glutathione, have been used previously to interface with biological systems. These MPCs are ideal for biological applications not only due to their water-solubility but also their small size (<5 nm). These characteristics are expected to enable easy biodistribution and clearance. In this article, we show an unexpected toxicity is associated with the tiopronin monolayer protected cluster (TMPC), making it incompatible for potential *in vivo* applications. This toxicity is linked to significant histological damage to the renal tubules, causing mortality at concentrations above 20 μM. We further show how the incorporation of poly ethylene glycol (PEG) by a simple place-exchange reaction eliminates this toxicity. We analyzed gold content within blood and urine and found an increased lifetime of the particle within the bloodstream due to the creation of the mixed monolayer. Also shown was the elimination of kidney damage with the use of the mixed-monolayer particle via Multistix analysis, MALDI-TOF MS analysis, and histological examination. Final immunological analysis showed no effect on white blood cell (WBC) count for the unmodified particle and a surprising increase in WBC count with the injection of mixed monolayer particles at concentrations higher than 30 μM, suggesting that there may be an immune response to these mixed monolayer nanoparticles at high concentrations; therefore, special attention should be focused on selecting the best capping ligands for use *in vivo*. These findings make the mixed monolayer an excellent candidate for further biological applications using water-soluble nanoparticles.

Introduction

Monolayer protected clusters (MPCs) consist of a small (<5 nm) metallic core surrounded by a monolayer of various ligands (*1*−*6*). The properties of these nanoscale molecules have been studied extensively including electrochemical (*7*), luminescent (*8*), and overall characterization (*9*). In particular, the ability to modify their chemical properties as a function of size is extremely useful in the fields of chemistry and nanoscale science (*10*). The ability to incorporate multiple, diverse, functional groups onto the nanoparticle via place-exchange reactions or amide coupling leads to multifunctional nanoparticles which have gained much attention (*8*), specifically, for the ability to incorporate peptide mimics within the monolayer. Previous studies from the Cliffel laboratory have shown that the incorporation of peptide epitopes can induce antibody binding to the nanoparticle as if it were the antigen (*11, 12*), while the Feldheim group has explored the use of water-soluble gold MPCs for the applications of gene delivery (*13*) and cellular internalization (*14*). Also noteworthy are the developments from the Hainfeld group using gold nanoparticles to enhance radiotherapy (*15, 16*). Their intravenous injections of 1.9 nm gold particles produced an increase in survival rate among mice bearing mammary carcinomas versus those given normal X-ray treatment. Their study also showed no apparent toxicity from the nanoparticles and a large rate of clearance through the kidneys.

Previous literature accounts show that nanoparticles exhibit toxicity due to a process known as opsonization or immune targeting within the body (*17*−*20*). When opsonization occurs, the target is engulfed by phagocytes and eliminated by the immune system. It has been shown that charged particles are extremely susceptible to the opsonization process, specifically opsonization by proteins (*17*). Proteins adhere to the charged surface of the particle, creating a layering effect, thus increasing the hydrodynamic radius significantly. The additional layering of protein is a large enough increase in the hydrodynamic radius to disable smooth clearance within the body. The mechanism for the phagocytosis of opsonized nanoparticles has been shown to be receptor-mediated (*18*). Essentially, the particles become lodged or cause substantial damage as they attempt to pass through the body. If this occurs, the nanoparticle is essentially useless for biological applications due to either substantial damage to the organs or in most cases, death of the organism. Therefore, it is thought that smaller particles with lower charge density on their surface ligands can escape the opsonization process and lower the clearance time of the particle. A hydrodynamic size over 15 nm has been shown to cause toxic effects *in vivo* (*21*). In Choi et al., a series of cadmium selenium quantum dots were tested *in vivo* for clearance and distribution rates; their findings show a negative correlation between hydrodynamic size and clearance. Specifically, they calculated the hydrodyamic range for rapid, immediate clearance to be <5.5 nm; they also calculated the hydrodynamic range for prevention of clearance to be >15 nm. Therefore, the ideal range for *in vivo* experiments in order to avoid immediate clearance or biological damage/lodging of the particle is 5 nm < x < 15 nm.

* To whom correspondence should be addressed. E-mail: david.e.cliffel@vanderbilt.edu.

[†] Current address: Department of Chemistry and Industrial Hygiene, University of North Alabama, Florence, Alabama 35630.

[‡] Current address: Department of Chemistry and Physics, Emmanuel College, Boston, Massachusetts 02115.

10.1021/tx100209t
Published on Web 07/22/2010

In vitro, cellular studies have looked at the effects of surface properties (*22*) such as charge (*23*) on nanoparticle entry through the plasma membrane, but no correlation between *in vitro* and *in vivo* toxicity has been demonstrated so far.

Our study focuses on the effects of the tiopronin monolayer protected cluster (TMPC) in a murine model. The TMPC is composed of two nontoxic materials (Au^0 core and tiopronin coating), both of which are routinely used for *in vivo* applications. The ligand, tiopronin, is commonly used under the trade name Thiola (*24*−*26*) to treat chronic diseases such as hepatic disease and cystinuria, while low concentration gold complexes are routinely given as rheumatoid arthritis injections. Given the components of the TMPC and its nanometer size, toxicity is not expected; however, the TMPC is charged, and thus could be susceptible to opsonization. For this reason, it may be necessary to modify the particle to withstand this process. Luckily, TMPCs are capable of undergoing simple place-exchange reactions to modify their monolayers to improve functionalization and lower the overall charge density to allow the particles to escape the opsonization process.

There have been many documented studies on the incorporation of PEG to reduce toxicity *in vivo*, particularly polymeric species as well as nanoparticles (*14, 19, 27*−*33*). These studies show that the incorporation of PEG increases the circulation half-life of the species within the bloodstream. To ensure an increase in the circulation half-life, PEG chain length as well as particle/polymer size must be considered. For example, a study by the Feldheim group focusing on four distinct nanoparticle diameters as well as three distinct PEG chain lengths demonstrated how these factors influenced cellular internalization (*14*). Using mixed-monolayer gold particles containing a receptor mediated endocytosis (RME) peptide and poly ethylene glycol exchanged onto citrate gold nanoparticles, their cellular studies showed that stability increased with decreasing nanoparticle diameter and increasing PEG chain length. Also shown was no significant difference between long PEG chain lengths (PEG 5000) and shorter lengths (PEG 900) with regard to cell internalization hindrance, as would be expected. The results further exemplify that smaller nanoparticles are the best choice for biological nanoparticle experimentation, and PEG allows for easier cellular internalization.

Moghimi et al. showed that particles with a large hydrodynamic radius (>200 nm) exhibited a more rapid rate of clearance than those of a small radius, regardless of PEG-ylation. However, regardless of size, PEG did aid in the clearance time of all particles; therefore, PEG-ylation is necessary to ensure the longest possible clearance time. Another trend noted by Gref et al. is that PEG-ylated PLA particles shift the biodistribution to the spleen rather than the liver as was seen with naked or non-PEG-ylated particles, indicating a possible immune response to the particle.

Of particular importance is the PEG-ylated species' ability to reduce interactions with proteins through hydrophilicity and steric repulsion, reducing opsonization. Gref et al. clearly showed that the addition of PEG to a PLA nanoparticle significantly increased blood residence time, allowing for better targeting. It has also been shown that PEG-ylation of gold nanorods significantly enhanced blood circulation time and exhibited no cytotoxicity *in vitro* (*34*). Further examination of the gold nanorods *in vivo* showed circulation within the blood up to 72 h postinjection and a huge concentration of nanorod within the liver at 72 h postinjection. Other studies include *in vitro* applications of gold nanoparticles through rat skin and intestine, showing that smaller nanoparticles had a wider distribution (*35*). Both studies involved particles/rods on a large size scale (>15 nm); previous evaluation of gold nanoparticles at smaller sizes has been limited. Therefore, the investigation of toxic effects (if any) shown by a small size (<5 nm) PEG-ylated particle is needed. We have chosen to incorporate PEG into our TMPC monolayer to deduce if this will reduce or eliminate the toxic effects shown previously.

While the incorporation of the PEG into the monolayer should produce positive results for the TMPC study, the literature also cites development of an antibody to the PEG species at high concentrations (*36*−*42*). Armstrong et al. first reported on a natural occurrence of the anti-PEG antibody within a normal blood donor sample at ca. 25% (*37*). They have also shown that the antibody adversely affects the clearance rate of PEG-ylated species, specifically PEG-asparaginase (*36*). The rapid clearance is due to an inherent immune response by the anti-PEG antibody. The natural occurrence of this antibody could severely limit which subjects could benefit from PEG-ylated particle therapy. The anti-PEG antibody has also been shown when a large quantity of PEG is introduced *in vivo,* specifically with repeated injections of PEG-ylated species (*42*) as well as with one-time injections (*40*), dependent on the concentration. Particular attention should be paid to immune responses generated by the PEG-ylated species to elicit whether the antibody has been produced or possibly whether its occurrence is natural.

This study seeks to discover if TMPCs may be used as a scaffold for the *in vivo* development of multifunctional nanoparticles through the analysis of gold content within the blood, urine, and organs via inductively coupled plasma optical emission spectroscopy (ICP-OES), inductively coupled plasma mass spectrometry (ICP-MS), histological examination of the organs, and matrix-assisted laser desorption ionization time-of-flight mass spectrometry (MALDI-TOF MS) analysis of the urine for potential renal damage biomarkers. Final analysis of the immunogenic response was performed using a standard coulter counter to track red and white cell counts. The results demonstrate that renal damage occurs with TMPCs as synthesized but that this damage may be eliminated with the incorporation of PEG-thiol into the monolayer via place-exchange reaction.

Experimental Procedure

Reagents. Gold tetrachloroauric acid was synthesized in house from 99.99% gold shot. Tetrachloroauric acid trihydrate was synthesized according to the literature (*43*) and stored in the freezer at −20 °C. *N*-(2-Mercaptopropionyl)-glycine (tiopronin) (Sigma), (1-mercaptoundec-11-yl) tetra(ethylene glycol) (Sigma), Optima nitric acid (Fischer Scientific), methanol, acetic acid, deuterium oxide, Zapoglobin (Beckman Coulter), and Isoton dilutent (Beckman Coulter) were all used as received. Sterile phosphate buffered saline was purchased from Mediatech. A Millipore filtration system was used to obtain 18 MΩ water.

Synthesis of TMPC. TMPCs were synthesized by the traditional modified (*2*) Brust (*44*) reaction as prescribed in the literature. Briefly, to a 6:1 ratio (v/v) mixture of methanol and acetic acid was added tiopronin and tetrachloroauric acid trihydrate in a 3:1 (mol/mol) ratio. The reaction was carried out at 0 °C and allowed to stir for ∼30 min whereupon the solution was removed under vacuum. The remaining black solid was dissolved in 100 mL of water and adjusted to pH 1 with hydrochloric acid. The solution was then loaded into a cellulose ester dialysis membrane (MWCO = 10,000), placed in 4 L of water, and stirred continuously. The water was changed ca. every 12 h over a 1 week course. The solution was then removed under vacuum, and the resulting black nanoparticles were subsequently analyzed.

Place-Exchange of PEG. The tetra-EG chain was added to the TMPC via a place-exchange reaction as prescribed by the literature.

For maximum exchange, a ratio of 4:1 PEG/tiopronin (w/w) was applied. Briefly, 5 mg of TMPC was added to a 10 μL solution of 10 mg of PEG ligand in phosphate buffered saline (pH 7). The mixture was stirred for three days and centrifuged (MWCO = 3K) to remove any excess PEG ligand within solution. The particles were then analyzed for purity by the same means as the original TMPCs.

Nuclear Magnetic Resonance. ^{1}H NMR spectra were collected of highly concentrated ligand and nanoparticle samples on a Bruker AC400 MHz NMR spectrometer in deuterium oxide (D_2O).

Thermogravimetric Analysis (TGA). TGA was performed on all nanoparticle samples (ca. 5−10 mg) with a TGA 1000 instrument under N_2 flow (60 mL min^{-1}), recording data from 25 to 800 °C at a heating rate of 20 °C min^{-1}.

Transmission Electron Microscopy. The nanoparticles were prepared by adding ~1 mg of dried particle to 5 mL of DI water, sonicating for ~20 min, and then dropped for slow evaporation onto ultrathin carbon grids (400 mesh, Ted Pella, Inc.). Images were obtained with a Phillips CM20T operating at 200 keV with a calibrated magnification of 414 kX. Results are reported as the mean ± standard deviation obtained from the negatives using ImageJ software (NIH, http://rsb.info.nih.gov/ij/) using sample sizes of at least 50 particles from the TEM grid.

Animal Models. Animals were housed in a Vanderbilt Division of Animal Care (DAC) facility, fully certified by the Association for Assessment and Accreditation of Laboratory Animal Care (AALAC). Animals were housed under the supervision of full-time veterinarians and staff, with an approved IACUC protocol. BALBc/cAnNHsd mice, 5−6 weeks old, female, and weighing 15−16 g, were purchased from Harlan Laboratory. All animals were allowed one week for acclimation prior to experimentation. Nanoparticles were prepared in sterile saline buffer (n = 10 mice/concentration group) and injected subcutaneously. Subcutaneous injection is a more likely form of accidental administration as well as a primary method for vaccine development and results in a slower release into the animal. Initial studies also looked at intraperitoneal injections and noted no significant differences, and thus, subcutaneous injections were used in all reported studies. Dosage concentrations for TMPCs were 1.72, 3.44, 5.16, 6.88, 10.32, and 20.64 mg dissolved in 2.00 mL of PBS corresponding to approximate concentrations of 10, 20, 30, 40, 60, and 120 μM nanoparticles of which 200 μL was injected into each mouse. Dosage concentrations for PEG-TMPCs were 2.97, 5.96, 8.94, 11.91, and 17.87 mg dissolved in 3.00 mL of PBS corresponding to approximate concentrations of 10,20,30, 40, and 60 μM nanoparticles of which 200 mL was injected into each mouse. Blood was drawn via submandibular bleeding techniques, in compliance with our protocol and NIH bleeding guidelines for mL/kg body weight per 2 weeks (*45, 46*). Urine was collected on cellophane with special precaution to avoid fecal contamination (*47*). Four weeks postinjection, mice were euthanized via CO_2 asphyxiation, followed by cervical dislocation. Blood samples were divided among ICP-MS/ICP-OES and Coulter Counter, and organs were harvested for histology and trace metal analysis. Urine was tested both for gold content and biological indicators (see Urine Strip Analysis).

ICP-MS Analysis. Briefly, 5 μL of blood or urine was diluted in 10 mL of 2% nitric acid (Optima grade, Fisher Scientific). Organs were excised, weighed, and dissolved in concentrated nitric acid (70% HNO_3) and heated to dryness. The samples were then reconstituted in 10 mL of 2% nitric acid. Samples were then analyzed on ELAN DRC II ICP-MS.

ICP-OES Analysis. Fluid and tissue samples were prepared as ICP-MS measurements with minor modifications. After the 5 μL fluid samples and organs were suspended in 10 mL of 2% nitric acid, a 1:1 dilution with aqua regia (3:1 hydrochloric acid/nitric acid) was performed. From this combined solution, a 1 mL aliquot was taken and resuspended in 9 mL of 2% nitric acid for ICP-OES analysis. Spectra were collected on a Perkin-Elmer ICP-OES Optima 700 DV. Argon plasma flow was set to 15 L min^{-1} and nebulizer flow at 0.2 L min^{-1}. Pump flow was 1.5 mL min^{-1} with RF power at 1300 W. Spectra were collected at the best gold intensity wavelength, 267.595 nm, with a delay time of 40 s. Spectra were collected in triplicate and averaged for final gold content analysis. Data were reported as the average of 10 mice per time-point for 0, 2, and 4 weeks blood, urine, and organ values, respectively. For injection day values, each time-point for blood/urine was taken from one individual mouse. Because of regulations on animal bleeding, blood was only collected from each mouse once per week; therefore, an hourly sampling of each mouse was not possible.

Urine Strip Analysis of Urine. Urine was analyzed for blood, protein content, leukocytes, ketones, and glucose using commercially available MultiStix 10 SG Reagent Strips (Siemens, Tarrytown, NY). The concentration of each analyte was determined by the manufacturer's given color charts.

MALDI-TOF MS Analysis of Urine. Purification and Digestion. Urine was collected from 5 individual mice and combined for each MALDI-TOF MS sample. Extracted urine samples (approximately 40−60 μL) were desalted by C-18 spin columns (Pierce, Rockford, IL) according to the Pierce protocol. Purified proteins were proteolytically digested by trypsin. Protein concentrations were determined by MultiStix protein strips. Briefly, proteolysis was performed by taking 2.6 μg of protein and diluting to 25 μL with 25 mM ammonium bicarbonate. Cysteine sulfhydryl groups were reduced by the addition of 1.5 μL of 45 mM dithiothreitol (DTT) for 30 min at 55 °C followed by alkylation with 2.5 μL of 100 mM iodoacetamide for 30 min at room temperature in the dark. Digestion was performed using 100 ng (1:40 enzyme/substrate, wt/wt) of trypsin gold (Promega, Madison, WI) at 37 °C for 16 h. Proteolysis was quenched by adding 1 μL of 88% formic acid.

MS Preparation. The quenched digest was lyophilized and then reconstituted in 25 μL of 0.1% formic acid and 5 μL of 20 mg/mL dihydroxybenzoic acid in 50% methanol. The samples were spotted using the dried-droplet method.

Instrumentation. Spectra were obtained using a Voyager-DE STR (Applied Biosystems, Inc.) MALDI-TOF-MS instrument in the delayed extraction (DE), positive, reflector mode. Data analysis was performed using Data Explorer software, version 4.3 (Applied Biosystems, Foster City, CA). Peaks were matched *de novo* using the PeptideMass Program (ExPASy Proteomics Server, Swiss Institute of Bioinformatics).

Coulter Counter Analysis of Blood. Cell count analysis was performed on a Beckman Z1 Coulter Particle Counter. From whole blood samples, 20 μL of blood was diluted into 20 mL of Isoton II dilutent (Beckman Coulter) to create the WBC solution. Next, 200 μL of WBC was transferred to 19.8 mL of dilutent; this solution was used as prepared for the RBC counts. To the WBC solution was added 15 drops of Zap-Oglobin II lysing agent (Beckman Coulter). It was allowed to sit for 2 min, and then, WBC counts were collected.

Histology. Organs were excised shortly after euthanasia, and sections of kidney were immediately fixed in formalin, 10% neutral buffered with 0.03% eosin (Sigma-Aldrich), and given to Vanderbilt Immuno Histology Core for H&E staining. The resulting slides were subsequently interpreted with help from Dr. Ken Salleng, D.V.M., Vanderbilt Division of Animal Care.

Results and Discussion

Characterization of MPCs. TMPCs were characterized by traditional analysis as documented in previous reports (*2*); all characterizations may be found in Supporting Information. The NMR spectrum showed significant broadening, indicative of the presence of nanoparticles. TGA analysis was within the normal range for TMPCs, showing an organic loss of 19.5%. Final TEM analysis produced an average core diameter of 2.5 ± 1.0 nm, within the desired range as prescribed by Choi et al. (*21*) for optimum biological efficiency. This combined with the TGA analysis (value taken at 500 °C) yielded an estimated molecular formula of $Au_{295}Tio_{88}$.

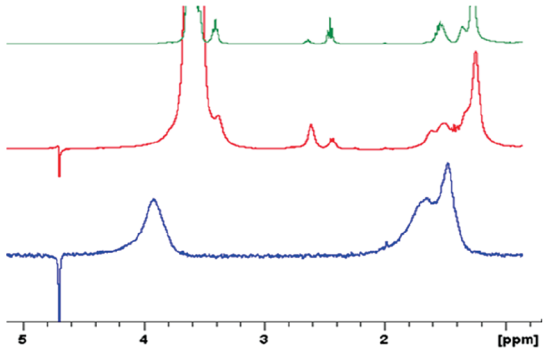

Figure 1. NMR comparison of PEG ligand (top), PEG-ylated TMPC (middle), and original TMPC (bottom). Signature line broadening is present in both the original TMPC and PEG-ylated TMPC spectra, signifying that the nanoparticles remained intact after place-exchange. Common to both the PEG ligand and the PEG-ylated TMPC are the two peaks at 2.5 ppm and 2.65 ppm, signifying that the TMPC was in fact PEG-ylated; the broadening of the signature PEG peaks denotes that the ligand is attached to the particle and not simply free in solution.

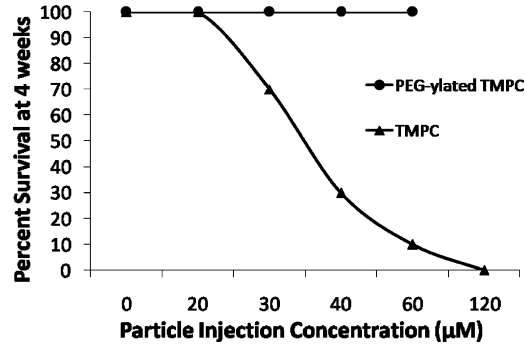

Figure 2. Morbidity comparison for TMPC study and study with PEG-ylated TMPC. Percent survival decreased at a relatively linear rate with increasing concentration for the original TMPC study. No morbidity was noted after the addition of PEG, and 100% survival was noted for all injected concentrations for the full 4-week study.

PEG-TMPCs were characterized by traditional analysis as well. Figure 1 shows the spectrum for the PEG ligand (top), the PEG-TMPC (middle), and the TMPC NMR spectrum (bottom). The peaks at 2.5 ppm and 2.65 ppm are common to both the PEG ligand as well as the PEG-ylated particle, proving that the particle was, in fact, PEG-ylated. The broadness of the peaks in the PEG-ylated spectrum suggests that the PEG was attached to the particle and is not free in solution. Unfortunately, with the presence of the alkyl-chain on the PEG ligand, quantitative analysis was not possible due to spectral overlap of the tiopronin and PEG ligands. Further study of quantification is currently underway. However, quantification was not necessary to prove that PEG-ylation of the particle did occur and to allow deduction of the improved toxicity from a PEG-TMPC.

TGA analysis of the PEG-TMPC may be found in Supporting Information. The analysis produced an organic loss of 72%, significantly higher than that of the TMPC. This large organic loss was not expected; the molecular weight of the PEG ligand was roughly twice that of the original tiopronin ligand (282.53 g/mol vs 163.19 g/mol). Therefore, the TGA results suggest that the PEG ligands not only exchange with the tiopronin ligands (as shown in the NMR spectrum) but also have a larger packing density, adding to the overall weight of the cluster. Final TEM analysis of the PEG-TMPC was performed to ensure that the particles did not collapse into polymeric species, as has been previously hypothesized. The micrographs of the TMPC and the PEG-TMPC may be found in Supporting Information. There was no significant difference noted in the cores of the nanoparticles, and no polymeric species were noted. The average size of the nanoparticle cores was assumed to have remained the same as before place-exchange.

MPC Biodistribution. Ultimately, the best assessment of nanotoxicity is morbidity. Shown in Figure 2 is the morbidity curve for both the TMPC synthesis and the PEG-TMPC. As is evident from the figure, no morbidity was seen at any concentration of the PEG-TMPC; while in comparison, morbidity was noted at all concentrations above 20 μM for the TMPC. This seems to show that the addition of PEG significantly improved the toxic effects of the tiopronin particle and eliminated any morbidity up to 60 μM. Given these findings, it became evident that PEG-ylation improved the clearance and biodistribution of the TMPC.

The biological toxicity of nanomaterials may be directly correlated to retention and clearance. One of the major clearance routes is renal filtration into urine. Urinalysis from the mice injected with both TMPCs and PEG TMPCs was conducted at specific time points to elicit gold concentration. These ICP-MS and ICP-OES plots may be found in Figure 3. For original TMPCs, the vast majority of the particle cleared in the first 8 to 24 h period for the lowest injected concentrations. For the 60 and 120 μM groups, the concentration drops dramatically from 10,000+ ppb to 100 ppb, which could indicate rapid clearance time. These groups also exhibited the highest mortality rates with 0% survival at 72 and 24 h, respectively. This could indicate that rapid clearance is detrimental to the renal system. Meanwhile, the groups exhibiting consistent clearance rates (0, 20, 30, and 40 μM) exhibited higher survival rates. Regardless, the concentration within urine returns to preinjection quantities of 1 to 20 ppb after 96 h. This indicates that the particle does eventually return to baseline levels.

The PEG-TMPC biodistribution within urine was relatively constant as opposed to the rapid clearance noted in the TMPC. Continued clearance indicates that there is no strain on the kidneys, nor is the renal system itself incapable of clearing the particle at a constant rate. The biodistribution for the PEG-TMPCs analysis was identical to that of the TMPC with the exception of the instrumentation used to analyze for gold content. For the PEG-TMPC, an ICP-OES instrument was used. The blank sample showed a 17 ppb gold concentration, and any value below this threshold was considered insignificant.

In addition to urine, blood was also analyzed for gold content. The analysis for the original TMPC blood may also be found in Figure 3. Parallel to the urine profile, a decrease is noted during the entire collection period, especially for the highest injected concentrations. This decrease correlates well with the urinalysis, as the filtration system has removed the bulk of the particles, leaving very little for circulation. Again, mice with the fastest decrease in concentration exhibited the most dramatic effects. The lower concentration groups (0 to 40 μM) had fairly uniform concentrations for the 24 h period. In-depth analysis could not be performed on the 120 μM group since the majority expired within 12 h, and it became necessary to euthanize the remaining subjects within 24 h. However, there was virtually no gold within the bloodstream of the samples collected, but extremely high gold content within the urine was found. This could be indicative of renal overload and stress.

From the distribution in the PEG-TMPC blood, the concentration of gold remains relatively constant for all concentrations, with no concentration value higher than 180 ppb. The only values that fall below the threshold are those obtained for the 0 μM saline control group; these values are, therefore, insig-

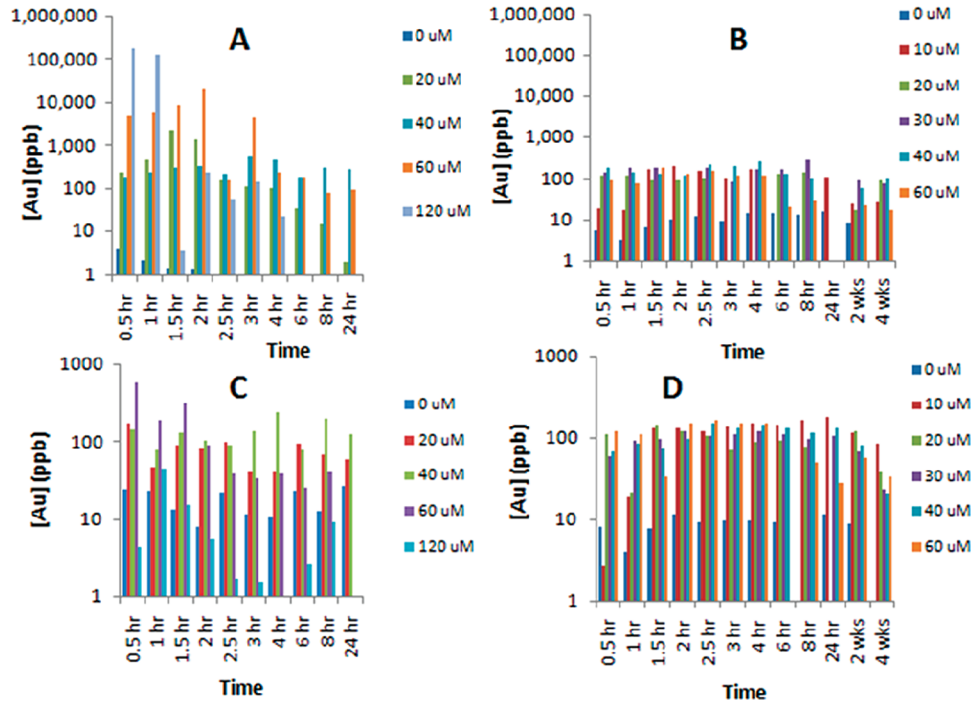

Figure 3. ICP-MS/ICP-OES elemental gold analysis of original TMPC urine (A) and blood (C) and PEG-ylated TMPC urine (B) and blood (D). One mouse subject was analyzed for each hourly time-point while an average of 10 mice was used for the 2 and 4 week time points for the PEG-ylated experiment. In the original TMPC experiment, the vast majority of TMPC is cleared within the first 8 h, with the exception of 120 μM. Those exhibiting steady clearance rates had the lowest mortality rates, while those who had rapid clearance (60 and 120 μM) expired quickly. Blood analysis correlated well with injected concentration, with the exception of 120 μM, which caused the mouse to not live long enough to complete the study. For the PEG-ylated TMPCs, blood analysis shows a consistent presence of particles within the blood even at 24 h postinjection for all concentrations. The 0 μM group is below the blank threshold and is considered relatively 0 ppb. Urine analysis exhibits a steady clearance of particles at all concentrations up to 24 h, implying that no renal damage has occurred as a result of the injection.

nificant, showing that the injection of the particle has an immediate effect. Also significant is the continual concentration within the blood. In the TMPC study, a high concentration was noted within 2 h of injection but was soon tapered within 24 h to relatively no gold observed. Previous studies have noted that the presence of PEG prolongs the presence of targeting molecules within the bloodstream; this blood biodistribution could be the result of the influence of the PEG ligand.

Because of the lack of morbidity, blood and urinalysis was performed at both 2 and 4 weeks postinjection for the PEG-TMPC subjects. Urine was collected from all mice, and an average value was taken for each concentration. These results are also shown in Figure 3. Analysis of the concentration within the blood and urine was also performed at 2 and 4 weeks. Again, the only values that fell below the threshold were those obtained for the 0 μM saline control group. In all distributions, the concentration within the blood at 2 weeks is only slightly smaller than the concentration seen on injection day; however, all concentrations also saw a decrease in concentration at the 4 week mark. It could be assumed that, given more time, the concentration would continue its decrease until the particle was completely cleared from the body. The gold concentration within the urine is somewhat inconsistent. Within most concentrations, there is a significant increase from week 2 to week 4, possibly indicative of rapid clearance after a prolonged period of time. In two cases (30 μM and 60 μM), there is a slight decrease from week 2 to week 4. However, if the gold concentration within the blood of these two injections is compared, it is relatively smaller than that in the other injections. It could be said that the clearance is lower because there was not as much particle to clear as opposed to the other injection concentrations, showing that clearance concentration is proportional to bloodstream concentration.

Another notable result is that the gold concentration within the blood and urine is higher in the lower injection concentrations (10 μM and 20 μM) than in the higher injection concentrations. This seems to indicate that the higher concentrations are being cleared more efficiently and quickly than the lower ones. Some work has shown that PEG-ylated species can induce an immune response at high concentrations. If the PEG-TMPCs are being targeted by the immune system at higher concentrations, clearance would be more rapid and efficient as opposed to normal transit through the bloodstream and renal system.

In addition to blood and renal clearance, the particles can also be retained within the organs. The main filtration organs are the kidneys and liver, while the spleen is blood-rich and important for recycling RBCs. The heart is also important due to heavy blood flow. For these reasons, these four organs were chosen for excision and examination. The results, which were corrected for differences in organ mass, show that the liver retains the most TMPCs followed by the spleen and kidney. Given the organs' primary function, this is presumed due to the liver's role in processing toxins, the spleen's role in recycling RBCs, and the kidney's role in filtering waste. The concentration of gold retained in the organs may be found in Supporting Information. All concentrations are relatively uniform with the exception of the 120 μM spleen; this is thought to be due to the quickness of euthanasia (24 h postinjection). This subject did not have the full four weeks the other mice had to fully clear the TMPCs from the spleen; given the full course of the study, perhaps the concentration would have been uniform.

For the PEG- TMPCs, the concentrations found within the saline group were essentially 0 μM and are not shown; only

one value fell at the threshold (10 μM liver). All organ concentrations obtained from the 20 μM injection are much higher in comparison to the other injection concentrations. All particles were extracted from the same synthesis batch, with the same average molecular formula; therefore, a size factor is not probable. All particles comprise the same materials and were synthesized from the same batch; therefore, a compositional problem is not probable, and since the injection concentration is so low, it is not probable that the amount is to blame. The only possibility is that the concentrations above 20 μM are experiencing a different clearance route, quite possibly due to an immune response within the body. An anti-PEG antibody has been noted within the literature and is associated with rapid clearance (*38*). The anti-PEG antibody was found in roughly 25% of a normal blood donor population (*37*), signifying that the antibody may be naturally occurring. Other reports cite the appearance of the anti-PEG antibody after high doses of a PEG-ylated species was introduced (*42*). It could, therefore, be interpreted that the rapid clearance after 20 μM is, in fact, due to an immunological response, most likely due to an anti-PEG antibody.

Barring the inclusion of 10 and 20 μM values, an ascending pattern is noted as a function of injection concentrations for both the liver and the heart, and a descending pattern is noted for the spleen as a function of injection concentration. The kidney shows no linearity; this is not surprising, however, due to different clearing rates within each mouse, time of last void, etc. The kidney values are, however, relatively close to each other. It could be stated that at concentrations above 20 μM, a linear pattern is noted for most critical organs based upon injection concentration. This is useful for future targeting aspects.

MPC Immunological Analysis. While gold concentration will elicit particle distribution throughout the body, there are biological factors that influence how the particle is expelled from the body and what effect (if any) the particle has on the body. One such factor is that of an immune response via the recruitment of WBC production. In order to assess whether the particle elicited an immune response, WBC and RBC counts were monitored via a standard Coulter counter at 0, 2, and 4 week time points to evaluate acquired immunity due to injection of the nanoparticle and analyzed as the ratio of RBC count/WBC count for better representation of the whole blood sample. These results are shown in Figure 4. The cell counts indicate that the TMPC does not cause a statistically relevant change in RBC or WBC counts, or their ratio during the four-week study for any of the injected concentrations. Given these findings, it may be assumed that the TMPC is immunogenetically silent; that is, it will not cause an immune response *in vivo.*

For PEG-ylated TMPCs, no discernible increase in white count is noted at concentrations below 30 μM. All WBC and RBC ratios are statistically insignificant (within 95% confidence level) and consistent with the original TMPC study, suggesting that there is no immunological response to the PEG-ylated TMPC at low concentrations.

The ratio counts for 30 μM remain relatively consistent during the 4 week period, signifying no change in the WBC count, yet high concentrations (40 and 60 μM) produce a linearly decreasing, statistically significant (asterisked, $p < 0.01$) pattern of the RBC/WBC ratio over the 4 week period, reflecting a surprising increase in WBC count. This increase in WBCs is most likely due to an immunological response to the incorporation of the poly ethylene glycol. Previous studies have shown that high concentrations of PEG will produce antibodies and trigger an immune response (*42*). An immunological reaction to the PEG-TMPC may explain the increase in clearance time for the higher injection concentrations. If the particles are being targeted by the immune system, they will be cleared faster than those subjected to simple renal filtration. Again, this is most likely attributable to an anti-PEG antibody.

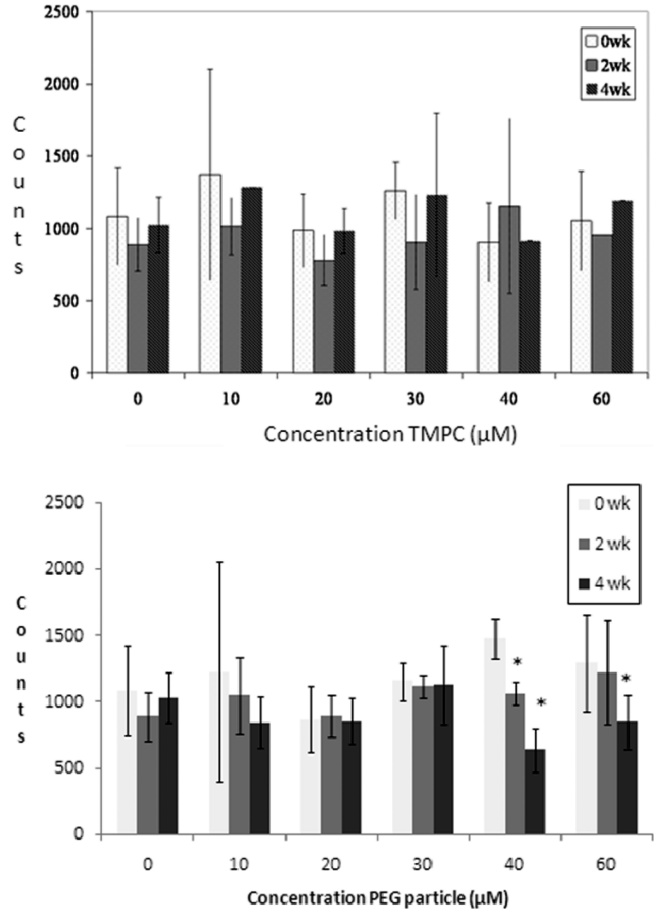

Figure 4. Coulter Counter analysis for original TMPC (top) and PEG-ylated TMPC (bottom). Graphical representation of ratio of RBC count: WBC count. No statistically relevant change is noted in the RBC or WBC count or their ratio; therefore, it may be assumed that the TMPC does not invoke an immune response at any concentration. However, a noticeable increase in WBC count is shown at concentrations of 40 and 60 μM for the PEG-ylated TMPCs, indicating an immune response at high concentrations. Asterisk indicates significantly different values ($p < 0.01$).

MPC Histology. Final evaluation of the TMPC study was conducted on kidney tissue samples via histological analysis at the Division of Animal Care at Vanderbilt University; the H&E stains obtained for the saline, 20 μM, and 40 μM group samples are shown in Figure 5A. At 20 μM TMPC injection, there is less renal damage; however, shedding and necrosis are still present. The 40 μM mice experience severe renal damage, extreme shedding of the epithelium/tubules, and mineralization. Both subjects were essentially in acute renal failure. Only the saline group showed no damage to the kidney tissue. Upon histological analysis, it was deemed that the TMPC was no longer an option for *in vivo* experimentation due to potential renal complications, morbidity at almost all concentrations, and the advice of the veterinary staff. It then became necessary to modify the particle to prevent renal damage and allow safe circulation *in vivo* to continue our experimental progression.

After modification with PEG, histological examination was performed to assess renal damage from the new nanoparticle.

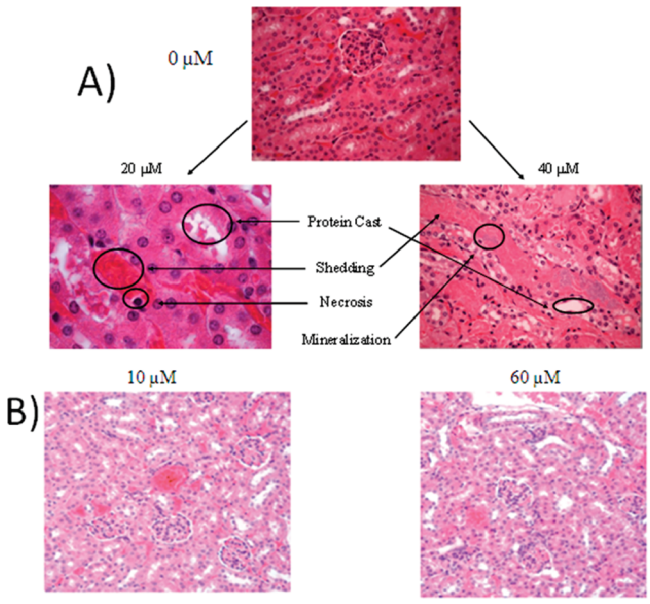

Figure 5. Representative histology slides of 0, 20, and 40 μM injection subjects for original TMPC injection (A) and histological slides of 10 μM and 60 μM injection of PEG-lyated particle mice kidneys (B). Obvious renal damage is noted for both TMPC injected subjects, with a correlative increase in damage with an increase in injection concentration. No damage was noted for the saline control group or for either concentration of PEG-ylated particle, showing the PEG-ylated particle eliminated the renal damage produced by the original TMPC.

These slides for the lowest (10 μM) and highest (60 μM) injected concentrations may been seen in Figure 5B. From the stains, no discernible damage is noted for either concentration. There are no protein casts present, and no shedding is observed. Both stains were deemed to have no discernible damage and deemed healthy by our veterinarian. This final confirmation suggests that the PEG-ylation of the TMPC essentially eliminates all traces of toxicity previously seen for the unmodified TMPC. We also note that the PEG-TMPC is expected to be a slightly larger hydrodynamic diameter (approximates are 5 nm TMPC vs 6 nm PEG-TMPC), but still well within the expected range for easy kidney filtration.

Analysis of Renal Clearance. Our previous study denoted extreme damage to the renal system as a result of the TMPC injections. This was presumably the reason for the high mortality rates seen at most injection concentrations. These mortality rates were not seen with the new PEG-TMPC; however, it was critical to assess renal clearance within the new mice to ensure that the particle was not causing sustainable damage. Using a conventional urinalysis strip, Multistix, urine from mice at all concentrations was analyzed for protein, blood, glucose, ketones, and leukocytes. The results table of the Multistix analyses for the mice injected with the PEG-TMPC at all concentrations may be found in Supporting Information. From the analyses, no glucose, blood, or leukocytes was present in any samples during the entire experiment, signifying that no WBCs, RBCs, or sugars were present within the urine. There was an occurrence of ketones within the 20 μM group between 2 and 3 h. The presence of ketones in urine generally signifies starvation or acidosis; however, there are no ketones present beyond this time point, nor are there ketones present within any other concentration at any time point. The two readings account for two mice at two time points; it may be assumed that those readings were isolated cases as no other mice displayed ketones, nor did those mice display ketones at any point beyond that reading, or that it was a misinterpretation of the color on the strip by the examiners.

Analysis of the protein content shows a relatively low/moderate concentration present even before the injection; small quantities of protein within the urine are considered normal. No discernible change is noted for 0−40 μM species, which is remarkably different from the previous study in which extremely high protein content was noted at every concentration, representative of the renal damage inflicted by the particle. Here, no protein is noted, presumably because no renal damage is being caused by the PEG-TMPC. The 60 μM concentration does show a spike to high protein content around 4 h postinjection; however, the content rapidly declines to low at 8 h; therefore, this could be deemed a normal occurrence or simply an error reading the strip. It can be assumed through this analysis that (1) damage signified by protein within the urine, most likely the formation of protein casts due to renal shedding, has been eliminated with the incorporation of PEG and that (2) the urine shows none of the effects that would be expected as a result of renal failure/damage even at 2 weeks postinjection.

To further test for renal damage, peptide mass mapping of proteins and peptides was performed on the urine by MALDI-TOF MS (*48*). Previous studies have successfully labeled biomarkers within the urine commonly seen as a result of renal damage/failure (*49*). The most common of these biomarkers is the presence of serum albumin; mouse serum albumin (MSA) is commercially available for testing. MSA should be present at some quantity within all urine samples experiencing renal damage. The results of the MALDI-TOF MS analysis of the urine for (a) the urine from mice injected with TMPCs with no modifications and (b) the urine from mice injected with the new PEG-TMPC may be found in Supporting Information. Biomarkers for MSA were noted in urine samples taken from the mice injected with TMPC nanoparticles, confirming renal damage as noted in both histology and urine strip analysis, while no markers for MSA were noted in the urine samples obtained from the mice injected with the PEG-ylated particles.

Conclusions. While its individual components are not toxic, the TMPC is not suitable for use *in vivo* in its native state; however, the incorporation of poly ethylene glycol onto the TMPC to form a mixed monolayer seems to essentially eliminate the toxicity. No discernible damage was noted for the renal system, and the particle was present within the blood and urine even 4 weeks postinjection at injection concentrations up to 60 μiM. Some immunological response was noted above 30 μM, presumably leading to the creation of an anti-PEG antibody; this should be considered for future TMPC immunological studies. Preferentially, to preclude any immune response to only the poly ethylene glycol ligand, concentrations of modified TMPC not exceeding 30 μM should be used to effectively test for immunity to other incorporations into the mixed monolayer. This being said, the PEG-TMPC appears to be an excellent candidate for future immunological studies *in vivo*.

Acknowledgment. We thank both Randi Gant-Branum and Dr. John A. McLean for their help with the MALDI-TOF MS analysis and Dr. Ken Salleng, DVM of the Division of Animal Care at Vanderbilt University, for all of the histological analysis and stains. We also thank the Vanderbilt Institute for Nanoscale Science and Engineering for use of the TGA

and TEM equipment. This work was made possible by a grant from the National Institutes of Health (R01 GM 076479).

Note Added after ASAP Publication. This paper was published on the Web on July 22, 2010. Text changes were made in the Animal Models paragraph of the Experimental Procedures section, the first paragraph in Characterization of MPCs of the Results and Discussion section, the last paragraph in MPC Biodistribution of the Results and Discussion, and the caption of Figure 4. The caption of Supporting Information Figure 1 was also updated. The corrected version was reposted on August 18, 2010.

Supporting Information Available: Full particle characterizations, MultiStix analysis, ICP-MS, and ICP-OES. This material is available free of charge via the Internet at http://pubs.acs.org.

References

(1) Templeton, A. C., Wuelfing, W. P., and Murray, R. W. (2000) Monolayer-protected clusters. *Acc. Chem. Res. 33*, 27–36.

(2) Templeton, A. C., Chen, S., Gross, S. M., and Murray, R. W. (1999) Water-soluble, isolable gold clusters protected by tiopronin and coenzyme A monolayers. *Langmuir 15*, 66–76.

(3) Whetten, R. L., Khoury, J. T., Alvarez, M. M., Murthy, S., Vezmar, I., Wang, Z. L., Stephens, P. W., Cleveland, C. L., Luedtke, W. D., and Landman, U. (1996) Nanocrystal gold molecules. *Adv. Mater. 8*, 428–433.

(4) Jadzinsky, P. D., Calero, G., Ackerson, C. J., Bushnell, D. A., and Kornberg, R. D. (2007) Structure of a thiol monolayer-protected gold nanoparticle at 1.1 Angstrom resolution. *Science 318*, 430–433.

(5) Whetten, R. L., and Price, R. C. (2007) Nano-golden order. *Science 318*, 407–408.

(6) Hostetler, M. J., Wingate, J. E., Zhong, C.-J., Harris, J. E., Vachet, R. W., Clark, M. R., Londono, J. D., Green, S. J., Stokes, J. J., Wignall, G. D., Glish, G. L., Porter, M. D., Evans, N. D., and Murray, R. W. (1998) Alkanethiolate gold cluster molecules with core diameters from 1.5 to 5.2 nm: core and monolayer properties as a function of size. *Langmuir 14*, 17–30.

(7) Cliffel, D. E., Zamborini, F. P., and Murray, R. W. (2000) Mercaptoammonium monolayer protected, water-soluble gold, silver, and palladium clusters. *Langmuir 16*, 9699–9702.

(8) Templeton, A. C., Cliffel, D. E., and Murray, R. W. (1999) Redox and fluorophore functionalization of water-soluble, tiopronin-protected clusters. *J. Am. Chem. Soc. 121*, 7081–7089.

(9) Templeton, A. C., Hostetler, M. J., Kraft, C. T., and Murray, R. W. (1998) Reactivity of monolayer-protected gold cluster molecules: steric effects. *J. Am. Chem. Soc. 120*, 1906–1911.

(10) Shon, Y.-S., Mazzitelli, C., and Murray, R. W. (2001) Unsymmetrical disulfides and thiol mixtures produce different mixed monolayer-protected gold clusters. *Langmuir 17*, 7735–7741.

(11) Gerdon, A. E., Wright, D. W., and Cliffel, D. E. (2005) Hemagglutinin linear epitope presentation on monolayer-protected clusters elicits strong antibody binding. *Biomacromolecules 6*, 3419–3424.

(12) Gerdon, A. E., Wright, D. W., and Cliffel, D. E. (2006) Epitope mapping of the protective antigen of *B. anthracis* by using nanoclusters presenting conformational peptide epitopes. *Angew. Chem. Int. Ed. 45*, 594–598.

(13) Tkachenko, A. G., Xie, H., Coleman, D., Glomm, W., Ryan, J., Anderson, M. F., Franzen, S., and Feldheim, D. L. (2003) Multifunctional Gold Nanoparticle-Peptide Complexes for Nuclear Targeting. *J. Am. Chem. Soc. 125*, 4700–4701.

(14) Liu, Y., Shipton, M. K., Ryan, J., Kaufman, E. D., Franzen, S., and Feldheim, D. L. (2007) Synthesis, stability, and cellular internalization of gold nanoparticles containing mixed peptide-poly(ethylene glycol) monolayers. *Anal. Chem. 79*, 2221–2229.

(15) Hainfeld, J. F., Slatkin, D. N., Focella, T. M., and Smilowitz, H. M. (2006) Gold nanoparticles: a new X-ray contract agent. *Br. J. Radiol. 79*, 248–253.

(16) Hainfeld, J. F., Slatkin, D. N., and Smilowitz, H. M. (2004) The use of gold nanoparticles to enhance radiotherapy in mice. *Phys. Med. Biol. 49*, 309–315.

(17) Owens, D. E., III, and Peppas, N. A. (2006) Opsonization, biodistribution, and pharmacokinetics of polymeric nanoparticles. *Int. J. Pharm. 307*, 93–102.

(18) Alexis, F., Pridgen, E., Molnar, L. K., and Farokhzad, O. C. (2008) Factors affecting the clearance and biodistribution of polymeric nanoparticles. *Mol. Pharmaceutics 5*, 505–515.

(19) Moghimi, S. M., Hunter, A. C., and Murray, J. C. (2001) Long-Circulating and target-specific nanoparticles: theory to practice. *Pharmacol. Rev. 53*, 283–318.

(20) Chen, Z., Meng, H., Xing, G., Chen, C., Zhao, Y., Jia, G., Wang, T., Yuan, H., Ye, C., Zhao, F., Chai, Z., Zhu, C., Fang, X., Ma, B., and Wan, L. (2006) Acute toxicological effects of copper nanoparticles in vivo. *Toxicol. Lett. 163*, 109–120.

(21) Choi, H. S., Liu, W., Misra, P., Tanaka, E., Zimmer, J. P., Ipe, B. I., Bawendi, M. G., and Fangioni, J. V. (2007) Renal clearance of quantum dots. *Nat. Biotechnol. 25*, 1165–1170.

(22) Verma, A., and Stellacci, F. (2010) Effect of surface properties on nanoparticle-cell interactions. *Small 6*, 12–21.

(23) Arvizo, R. R., Miranda, O. R., Thompson, M. A., Pabelick, C. M., Bhattacharyya, R., Robertson, J. D., Rotello, V. M., Prakash, Y. S., and Mukherjee, P. (2010) Effect of nanoparticle surface charge at the plasma membrane and beyond. *Nano. Lett. 10*, 2543–2548.

(24) Shaw, C. F. (1999) Gold-based therapeutic agents. *Chem. Rev. 99*, 2589–2600.

(25) Devi, P. U., and Saharan, B. R. (1978) Chemical protection of mouse spermatocytes against gamma-rays with 2-mercaptopropionylglycine. *Experientia 34*, 91–92.

(26) Atamaca, G. (2004) Antioxidant effects of sulfur-containing amino acids. *Yonsei Med J. 45*, 766–788.

(27) Gref, R., Domb, A., Quellec, P., Blunk, T., Muller, R. H., Verbavatz, J. M., and Langer, R. (1995) The controlled intravenous delivery of drugs using PEG-coated sterically stabilized nanospheres. *Adv. Drug Delivery Rev. 16*, 215–233.

(28) Gref, R., Luck, M., Quellec, P., Marchand, M., Dellacherie, E., Harnisch, S., Blunk, T., and Muller, R. H. (2000) 'Stealth' corona-core nanoparticles surface modified by polyethylene glycol (PEG): influences of the corona (PEG chain length and density) and of the core composition on phagocytic uptake and plasma protein absorption. *Colloid Surf., B 18*, 301–313.

(29) Kaul, G., and Amiji, M. (2002) Long-circulating poly(ethylene glycol)-modified gelatin nanoparticles for intracellular delivery. *Pharm. Res. 19*, 1061–1067.

(30) Meng, F. H., Engbers, G. H. M., and Feijen, J. (2004) Polyethylene glycol-grafted polysterene particles. *J. Biomed. Mater. Res., Part A 70A*, 49–58.

(31) Moghimi, S. M., Porter, C. J. H., Muir, I. S., Illum, L., and Davis, S. S. (1991) Non-phagocytic uptake of intravenously injected microspheres in rat spleen: influence of particle size and hydrophilic coating. *Biochem. Biophys. Res. Commun. 177*, 861–866.

(32) De Jong, W. H., Hagens, W. I., Krystek, P., Burger, M. C., Sips, A. J. A. M., and Geertsma, R. E. (2008) Particle size-dependent organ distribution of gold nanoparticles after intravenous administration. *Biomaterials 29*, 1912–1919.

(33) Herold, D. M., Das, I. J., Stobbe, C. C., Iyer, R. V., and Chapman, J. D. (2000) Gold microspheres: a selective technique for producing biologically effective dose enhancement. *Int. J. Radiat. Biol. 76*, 1357–1364.

(34) Niidome, T., Yamagata, M., Okamoto, Y., Akiyama, Y., Takhashi, H., Kawano, T., Katayama, Y., and Niidome, Y. (2006) PEG-modified gold nanorods with a stealth character for in vivo applications. *J. Controlled Release 114*, 343–347.

(35) Sonavane, G., Tomoda, K., Sano, A., Ohshima, H., Terada, H., and Makino, K. (2008) In vitro permeation of gold nanoparticles through rat skin and rat intestine: effect of particle size. *Colloids Surf., B 65*, 1–10.

(36) Armstrong, J. K., Hempel, G., Koling, S., Chan, L. S., Fisher, T. C., Meiselman, H. J., and Garratty, G. (2007) Antibody against poly(ethylene glycol) adversely affects PEG-asparaginase therapy in acute lymphoblastic leukemia patients. *Cancer 110*, 103–111.

(37) Armstrong, J. K., Leger, R., Wenby, R. B., Meiselman, H. J., Garratty, G., and Fisher, T. C. (2003) Occurence of an antibody to poly(ethylene glycol) in normal donors. *Blood 102*, 556A.

(38) Armstrong, J. K., Meiselman, H. J., Wenby, R. B., and Fisher, T. C. (2003) In vivo survival of poly(ethylene glycol)-coated red blood cells in the rabbit. *Blood 102*, 94A.

(39) Leger, R. M., Arndt, P., Garratty, G., Armstrong, J. K., Meiselman, H. J., and Fisher, T. C. (2001) Normal donor sera can contain antibodies ot polyethylene glycol (PEG). *Transfusion 41*, 29S.

(40) Richter, A. W., and Akerblom, E. (1983) Antibodies against polyethylene glycol produced in animals by immunization with monomethoxy polyethylene glycol modified proteins. *Int. Arch. Allergy Appl. Immunol. 70*, 124–131.

(41) Richter, A. W., and Akerblom, E. (1984) Polyethylene glycol reactive antibodies in man: titer distribution in allergic patients treated with monomethoxy polyethylene glycol modified allergens or placebo, and in healthy blood donors. *Int. Arch. Allergy Appl. Immunol. 74*, 36–39.

(42) Sroda, K., Rydlewski, J., Langner, M., Kozubek, A., Grzybek, M., and Sikorski, A. F. (2005) Repeated injections of PEG-PE liposomes generate anti-PEG antibodies. *Cell. Mol. Biol. Lett. 10*, 37–47.
(43) Brauer, G., Ed. (1965) *Handbook of Preparative Inorganic Chemistry*, 1st ed., Academic Press, New York.
(44) Brust, M., Fink, J., Bethel, D., Shiffrin, D. J., and Whyman, R. (1994) Synthesis of thiol-derivatised gold nanoparticles in a two-phase liquid-liquid system. *J. Chem. Soc. Chem. Commun.* 801.
(45) Golde, W. T., Gollobin, P., and Rodriguez, L. L. (2005) A rapid, simple, and humane method for submandibular bleeding of mice using a lancet. *Lab Anim. 34*, 39–43.
(46) NIH (2005) *Guidelines for Survival Bleeding of Mice and Rats*. http://oacu.od.nih.gov/ARAC/Bleeding.pdf.
(47) Kurien, B. T., and Scofield, R. H. (1998) Mouse Urine collection using clear plastic wrap. *Lab. Anim. 33*, 83–86.
(48) Zerfos, P., Prados, J., Kossida, S., Kalousis, A., and Vlahou, A. (2007) Sample preparation and bioinformatics in MALDI profiling of urinary proteins. *J. Chromatogr. B 853*, 20–30.
(49) Coca, S. G., and Parikh, C. R. (2008) Urinary biomarkers for kidney injury: perspectives on translation. *Clin. J. Am. Soc. Nephrol. 3*, 481–490.

TX100209T